Random dilution effects in the frustrated spin chain β-$CaCr_{2-x}Sc_xO_4$

M. Songvilay,[1,*] S. Petit,[1] V. Hardy,[2] J. P. Castellan,[1,3] G. André,[1] C. Martin,[2] and F. Damay[1]
[1]*Laboratoire Léon Brillouin, CEA-CNRS UMR 12, 91191 Gif-sur-Yvette Cedex, France*
[2]*Laboratoire CRISMAT, CNRS UMR 6508, 6 Boulevard Maréchal Juin, 14050 Caen Cedex, France*
[3]*Institut für Festkörperphysik, Karlsruher Institut für Technologie, P.O. 3640, D-76021 Karlsruhe, Germany*
(Received 6 August 2014; revised manuscript received 22 January 2015; published 17 February 2015)

Random dilution effects in the magnetic zigzag ladder (J_1-J_2 chain) β-$CaCr_{2-x}Sc_xO_4$ have been investigated combining magnetic susceptibility, specific heat measurements, and neutron scattering. The pseudogapped magnetic excitations observed above T_N in β-$CaCr_2O_4$ ($x = 0$) persist up to $x = 0.3$ with an increasing characteristic frequency E_0 but vanish for $x = 0.5$ for which a quasielastic signal extending up to 8 meV becomes the characteristic feature of the magnetic spectrum. Magnetic ordering is seen up to $x = 0.3$ with decreased ordering temperature T_N and correlation length. The results are interpreted in terms of the progressive confinement of one-dimensional excitations within shorter chains as x increases and emphasize the crucial role of J_2 in propagating magnetic excitations. For an average chain length l smaller than ~16 magnetic atoms, the system breaks apart into a set of disconnected units with the dynamical properties of a spin glass.

DOI: 10.1103/PhysRevB.91.054408 PACS number(s): 75.10.Pq, 75.40.Gb, 75.45.+j

I. INTRODUCTION

Quantum effects are essential in the study of one-dimensional (1D) magnetism, and most theoretical or experimental investigations concentrate on compounds with either a spin $\frac{1}{2}$ or a spin 1. A comprehensively investigated case is the antiferromagnetic $S = \frac{1}{2}$ Heisenberg chain model, whose ground state lacks long-range magnetic order and which exhibits a gapless spectrum of elementary spinon excitations [1]. Among 1D half-integer spin systems, spin gaps in the excitation spectra can arise under special circumstances: in spin-Peierls compounds with a spontaneously dimerized ground state [2,3], in the case of frustrated exchange interactions with easy-plane magnetic anisotropy [4,5], asymmetric zigzag spin ladders [6], or two-leg ladders [7,8].

Very recently, the opening of a spin pseudogap has also been observed in a spin-$\frac{1}{2}$ chain compound, $SrCuO_2$, doped with 1% $S = 1$ Ni impurities [9], a result extended to other types of defects, such as spin vacancies or broken bounds, in magnetic chain systems. Effects of randomness can be particularly dramatic in quantum 1D magnets indeed, and a considerable amount of theoretical and experimental work has been devoted over the years to the study of random substitution effects [10–13]. In contrast with systems of higher dimensionality in which the host excitations can propagate around a vacancy, in one dimension their motion is completely blocked by vacancies [14]. This creates an assembly of finite-size chains [15] in certain cases leading to a modification of the low-energy excitation spectrum [16], experimentally observed in doped $SrCuO_2$ [9], and sometimes to a complete new ground state [17]. A striking illustration of the latter is the switching of the gapped spin liquid state to an antiferromagnetically ordered state which is induced by a 1% Zn substitution in $Sr(Cu_{1-x}Zn_x)_2O_3$ [18].

In this article, we address the case of random nonmagnetic substitution on the $S = 3/2$ zigzag ladder (inset of Fig. 1) β-$CaCr_2O_4$ [19]. β-$CaCr_2O_4$ exhibits long-range incommensurate cycloidal magnetic order below $T_N = 21$ K; above T_N, however, the inelastic neutron-scattering spectrum shows a magnetic signal [20], which is thought to arise from the contribution of a two-spinon continuum, in agreement with theoretical views on quantum frustrated chains within the $J_2 \gg J_1$ limit [1,21,22]. In contrast with the $S = \frac{1}{2}$ Heisenberg chain model, very little is actually known on random dilution effects on a frustrated chain. Static and dynamic disorder effects have been studied in the systems β-$CaCr_{2-x}Ga_xO_4$ and β-$Ca_{1-y}Cr_2O_4$, respectively, by Dutton *et al.* [23] and highlighted the crucial role of the type and nature of the dopant on the magnetic behavior observed. Here we report on the case of Sc substitution. Combining macroscopic physical measurements and neutron-scattering experiments on several β-$CaCr_{2-x}Sc_xO_4$ compositions ($0 \leqslant x \leqslant 1$), we show that, owing to the J_1-J_2 topology, the pseudogapped spectrum survives up to high dilution levels ($\leqslant 0.3$). It is argued that the confinement of the magnetic excitation within smaller magnetic segments can explain its high-frequency shift when x increases. Above $x \geqslant 0.5$, however, the ground state changes to that of a magnetic glasslike system.

II. EXPERIMENT

Polycrystalline β-$CaCr_{2-x}Sc_xO_4$ compounds were prepared by high-temperature solid-state reactions from stoichiometric amounts of CaO, Cr_2O_3, and Sc_2O_3, ground together and pressed in the shape of pellets before being heated at 1500 °C for 12 h in a reducing gas flow (5% H_2 in Ar). Samples were checked by room-temperature x-ray diffraction and found to be single phase and of good crystallinity. Within the series, all compounds are orthorhombic, and structural isotypes of $CaFe_2O_4$ (*Pbnm* space group for $x = 0$ [24,19] to $x = 2$ [25]). There is a regular increase in the cell volume with increasing x, owing to the larger size of Sc^{3+} (0.745 Å) with respect to Cr^{3+} (0.615 Å) [26]. Increasing Cr-Cr distances are therefore a direct consequence of the Sc substitution: The Cr-Cr distance along c (which corresponds to the J_2 exchange path of the zigzag ladder schematized in the inset of Fig. 1) increases from ~2.97 Å for $x = 0$ to ~3.05 Å for $x = 1.0$ as illustrated

*manila.songvilay@cea.fr

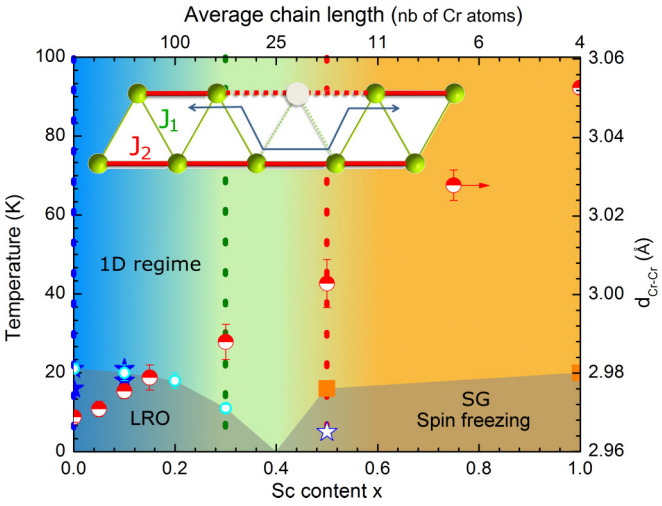

FIG. 1. (Color online) (x,T) phase diagram of the β-$CaCr_{2-x}Sc_xO_4$ series. Hollow light blue circles and filled blue stars indicate long-range magnetic order (LRO) transition temperatures (from neutron-diffraction and specific heat data, respectively). The orange squares correspond to the temperature below which an elastic magnetic scattering contribution can be seen on the neutron-scattering data (triple-axis measurements); the hollow blue star indicates the T_g of the $x = 0.5$ sample. Right scale (red and white circles): evolution of the Cr-Cr distance in the ladder legs along c (shown in red in the inset) at 300 K (from x-ray diffraction). The inset schematizes the substitution effect (gray circle) on a zigzag ladder, equivalent to a J_1–J_2 chain: For low substitution levels, impurities do not break the magnetic exchange path up to the second neighbor. For higher levels of substitution, defects can appear on two ends of a rung and break the ladder into smaller units.

in Fig. 1 (half-filled red circles, right scale). According to Rietveld refinement analyses of the neutron-diffraction data, the distribution of Sc, up to $x = 0.5$, is random within $\pm 3\%$.

dc magnetic susceptibility was derived from magnetization data recorded in a field of 100 Oe on warming from 2 to 300 K after a zero-field cooling (zfc) [physical property measurement system (PPMS), Quantum Design]. Additional investigation of the low-T regime ($T < 10$ K) was carried out in 10 Oe, both in the zfc and field-cooled cooling (fcc) modes using a superconducting quantum interference device magnetometer (magnetic property measurement system, Quantum Design). Complex ac susceptibility was measured in the frequency range of 10^1–10^4 Hz ($h_{dc} = 0$ and $h_{ac} = 10$ Oe), and isothermal $M(H)$ curves were measured at 2 K up to 9 T after a zero-field cooling (PPMS, Quantum Design). Zero-field heat-capacity measurements were carried out in the same device using a relaxation method with a 2τ fitting procedure. The magnetic specific heat C_{mag} was derived by subtracting the lattice contribution evaluated from the measurement of the nonmagnetic isomorph β-$CaSc_2O_4$.

Synchrotron x-ray diffraction was performed for the $x = 0$, 0.3, and 1 compounds on the CRISTAL beamline at SOLEIL ($\lambda = 0.72508$ Å). Neutron powder diffraction versus temperature was performed on the G4.1 diffractometer ($\lambda = 2.425$ Å) from 1.5 to 300 K, at LLB-Orphée (CEA-Saclay, France). Rietveld refinements were performed with programs of the FULLPROF suite [27]. Inelastic neutron scattering experiments were performed on the thermal triple-axis spectrometers 1 and 2 T ($k_f = 2.662$ Å^{-1}) at LLB-Orphée. Higher-order contaminations were removed with pyrolytic graphite; the energy resolution on both instruments for the given k_f is 2 meV.

III. RESULTS AND DISCUSSION

Figure 1 shows the (x,T) magnetic phase diagram of the β-$CaCr_{2-x}Sc_xO_4$ system as obtained from a comprehensive investigation of the $x = 0$, 0.1, 0.2, 0.3, 0.5, and 1 compositions using macroscopic physical properties and neutron-scattering measurements, which are detailed below.

The susceptibility versus temperature curve of β-$CaCr_2O_4$ ($x = 0$) is characterized by a broad maximum around 100 K, attributed to magnetic low dimensionality, with a subtle change in slope around $T_N = 21$ K when long-range magnetic ordering (LRO) sets in [19] [Fig. 2(a)]. Two magnetic transitions are actually seen on the specific heat curve $C(T)$ at 21 and 16 K [Fig. 2(b) and corresponding blue stars in Fig. 1], this second magnetic transition being understood as the transition from a spin-density wave with collinear moments to a cycloidal configuration with moments rotating on the ac plane [19].

As x is increased, the susceptibility curves [Fig. 2(a)] show a gradual smoothing of the broad feature at 100 K typical of the $x = 0$ compound, which is progressively replaced by a trend towards divergence as temperature is decreased. This overall behavior can be ascribed to the segmentation of the spin chains by the nonmagnetic Sc^{3+}, a process which rapidly decreases the impact of antiferromagnetic fluctuations along the surviving fragments of chains and eventually generates an increasing amount of "isolated" Cr^{3+} behaving as freelike spins.

As often encountered in quasi-1D systems, the magnetic long-range ordering transition temperatures are more clearly identifiable on the specific heat data than on the susceptibility curves. In Fig. 2(b), one observes that the two magnetic transitions reported for $x = 0$ are still present up to $x = 0.1$, even though in a narrower temperature range, at 17 and 20 K. In contrast, for $x = 0.3$ and above, these magnetic transitions are no longer discernible on the specific heat curves, whereas a broad bump emerges around 5 K for $x = 0.5$.

Additional magnetization measurements were performed for $x = 0.5$ in the low-temperature range with higher resolution in temperature (0.1 K) and in a smaller applied magnetic field (10 Oe). In Fig. 3(a), one clearly observes a peak on the zfc curve and a splitting between the zfc and the fcc data below this temperature (estimated to be 3.75 ± 0.05 K), a behavior known to be typical of a spin-glass (SG) state [28]. Several other features support the indication of a SG ground state in $x = 0.5$ for $T < T_g \sim 3.75 \pm 0.05$ K. First, for $x = 0.5$, a broad peak centered close to T_g is observed on the $C_{mag}/T(T)$ curve as expected for a SG state [28], whereas this feature is clearly absent for $x = 0$, whose ground state is LRO antiferromagnetic [Fig. 3(b)]. Second, the $M(H)$ curve of $x = 0.5$ at 2 K exhibits a rounded shape without any trend to saturation up to 9 T, the magnetization value at 9 T reaching only a small fraction of the calculated saturation (4.5 μ_B/f.u.) (where f.u. represents formula units). This behavior is also typical of spin glasses for $T < T_g$, and it strongly contrasts with the linear dependence expected for LRO antiferromagnetism, such as the one actually observed for $x = 0$ [Fig. 3(c)].

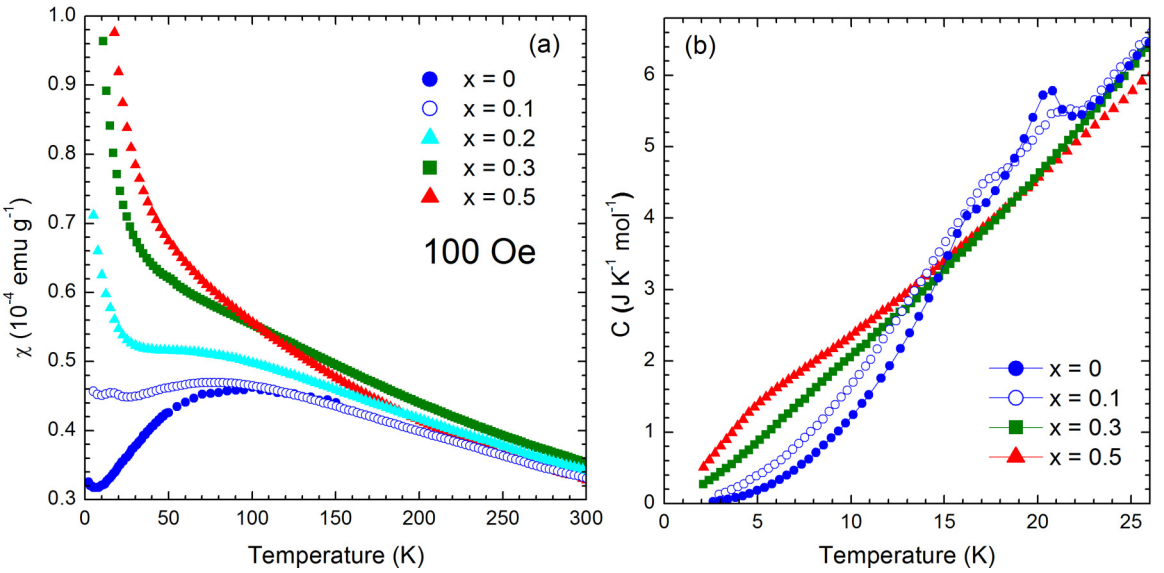

FIG. 2. (Color online) (a) Temperature evolution of the dc-magnetic susceptibility (in 100 Oe) of β-$CaCr_{2-x}Sc_xO_4$ compounds ($0 \leqslant x \leqslant 0.5$). (b) Temperature dependence of the specific heat for the $x = 0$, 0.1, 0.3, and 0.5 compounds.

To further probe the spin dynamics of the $x = 0.5$ sample, frequency-dependent susceptibility measurements were carried out. In Fig. 3(d), one observes that the temperature dependence of the real part of the susceptibility χ' exhibits a cusplike maximum at a temperature which increases as the frequency (f) is increased, which is precisely what is

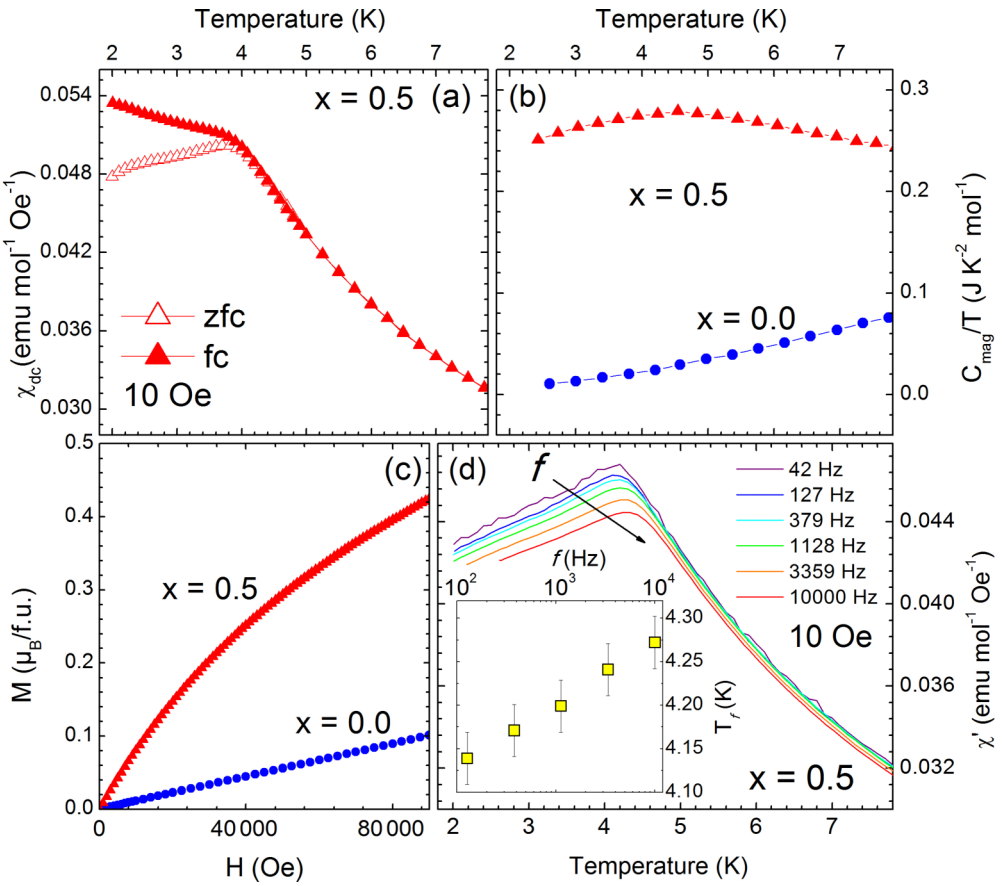

FIG. 3. (Color online) (a) dc susceptibility of β-$CaCr_{1.5}Sc_{0.5}O_4$ ($x = 0.5$) in 10 Oe after a zfc or fc process. (b) Temperature dependence of C_{mag}/T in 0 Oe and (c) field dependence up to 9 T of the magnetization M at 2 K for $x = 0$, 0.5 in the β-$CaCr_{2-x}Sc_xO_4$ series. (d) ac susceptibility of β-$CaCr_{1.5}Sc_{0.5}O_4$ ($x = 0.5$) versus temperature in 10 Oe at different frequencies in the $10^1 - 10^4$-Hz range. Inset: Corresponding frequency shift of the freezing temperature T_f versus frequency f.

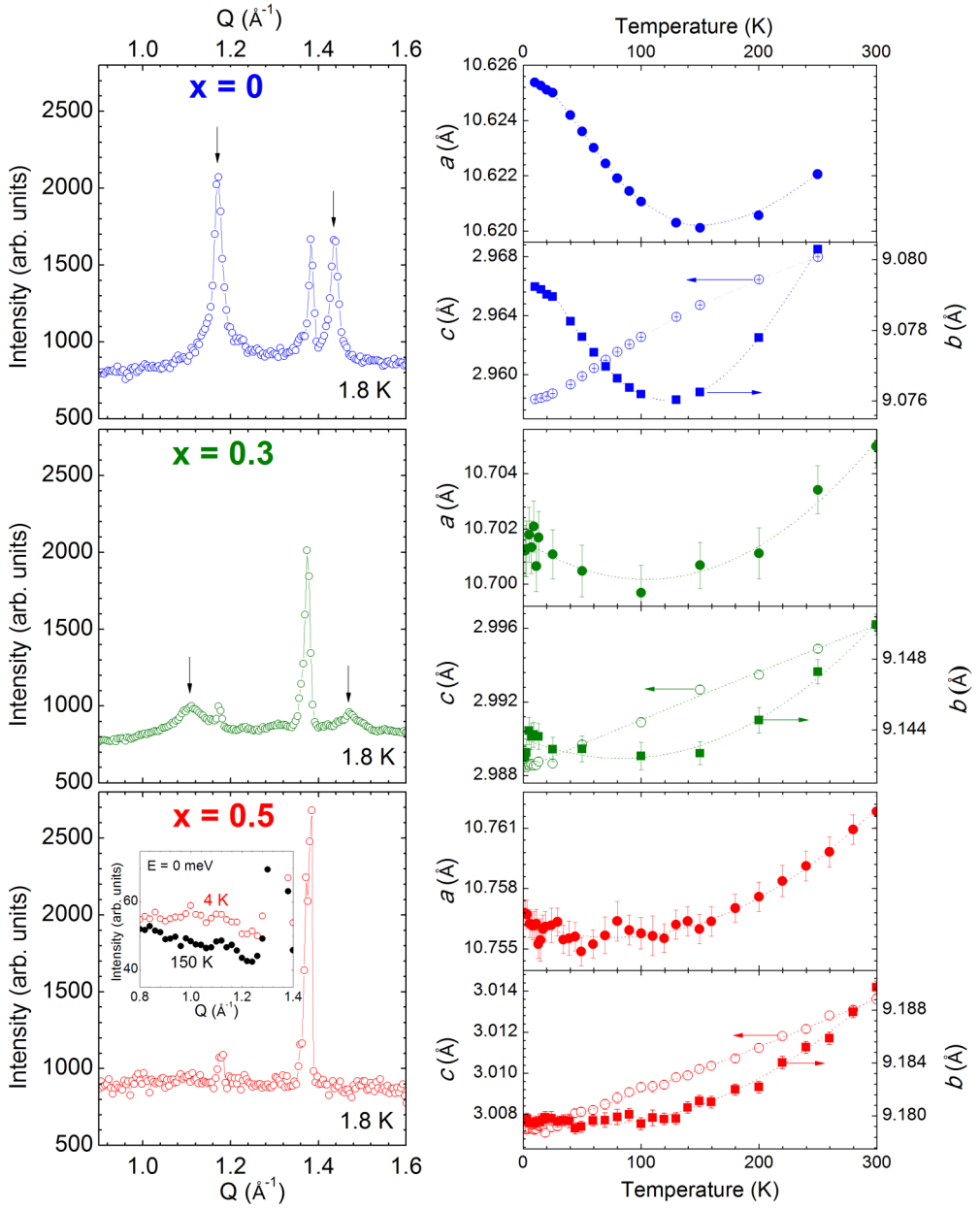

FIG. 4. (Color online) (Left) Neutron powder diffractograms at 1.8 K of $x = 0.0, 0.3$, and 0.5 β-$CaCr_{2-x}Sc_xO_4$ compounds (shown as blue, green, and red dotted lines, respectively, on the phase diagram of Fig. 1). Bragg magnetic peaks are identified by black arrows for $x = 0$ and 0.3. Inset: Elastic scans ($E = 0$ meV) at 4 and 150 K of the $x = 0.5$ compound. (Right) Temperature evolution of the a-, b-, and c-cell parameters (*Pbnm* space group) for the $x = 0, 0.3$, and 0.5 samples. For $x = 0$, the temperature dependence of the cell parameters has been extracted from synchrotron x-ray data and for $x = 0.3$ and 0.5, from neutron-diffraction data. Dotted lines are guide to the eyes.

expected for the freezing temperature $T_f(f)$ in a SG state [28]. More quantitatively, the relative shift of T_f per decade of frequency $[\Delta T_f/(T_f \Delta \log_{10}(f))]$ has a value of $\sim$0.017 [inset of Fig. 3(d)], which lies within the range typically found for spin glasses [28]. Finally, it can be noted that the $T_f(f)$ values found in the ac experiments are also consistent with the T_g ($\sim$3.75 K) previously estimated from dc measurements (i.e., long-time measurements corresponding to $f \to 0$).

Neutron diffraction was performed for several compositions of the β-$CaCr_{2-x}Sc_xO_4$ system to further investigate the evolution with x of the long-range magnetic ordering. The neutron diffractograms (Fig. 4, left panels) show that LRO is actually observed up to $x = 0.3$. The magnetic ordering temperature T_N decreases gradually with x as illustrated in Fig. 1 (hollow blue circles) and is accompanied by a significant decrease in both the magnetic correlation length and the ordered magnetic moment as x increases, in accordance with the fact that no transition is observed in the $C(T)$ data for $x \geqslant 0.3$. The magnetic correlation length determined from the width of the Bragg magnetic peak using the Scherrer formula [27] is down to

$\lambda = 80$ Å for $x = 0.3$ at 1.8 K. The component q of the magnetic propagation vector $\mathbf{k} = (0\,0\,q)$ also decreases regularly with the substitution, from $q = 0.477(1)$ for $x = 0$ to ~0.450(2) for $x = 0.3$ at 1.8 K. For $x \geqslant 0.5$, there is no sign of magnetic ordering, even short range, on the neutron-diffraction data down to 1.8 K. As shown in the inset of Fig. 4, nominally elastic- ($E = 0$ meV) scattering measurements on the $x = 0.5$ compound actually show a very weak magnetic contribution over a $1-1.2$ Å^{-1} Q range on the difference between 4 and 150 K data, as in the case of frozen magnetic disorder, a result consistent with the susceptibility and specific heat measurements.

In parallel, although the *Pbnm* symmetry is kept over the whole substitution range investigated, the magnetoelastic effect, which has been identified in β-$CaCr_2O_4$ [19] and which is characterized by a negative thermal expansion of the *a*- and *b*-cell parameters below 100 K, persists up to $x = 0.3$ but disappears for $x = 0.5$, for which it is replaced by a Debye-like contraction of the *a*-, *b*-, and *c*-cell parameters as temperature decreases [$a(T)$, $b(T)$, and $c(T)$ curves for $x = 0$, 0.3, and 0.5 are shown in the right panels of Fig. 4]. A low-temperature synchrotron x-ray investigation of the $x = 0$ compound confirms, in addition, the lack of structural transition or symmetry lowering down to 10 K.

To characterize the various magnetic regimes of the (x,T) diagram shown in Fig. 1, especially above T_N, where low-dimensional effects are expected, inelastic neutron-scattering experiments were performed at different temperatures for the $x = 0$, 0.2, 0.3, and 0.5 compositions. Representative maps of the inelastic-scattering spectra $S(Q,E)$ are shown in Fig. 5 for $x = 0.0$, 0.3, and 0.5 at $T \ll T_N$ (1.5 or 4 K) and $T \gg T_N$ (90 K). The corresponding temperature evolution of energy profiles at $Q = 1.25$ Å^{-1} (E scans) and of Q scans at constant energy transfer $E = 4$ meV are illustrated in Fig. 6 (left and right panels, respectively).

The excitation spectrum of β-$CaCr_2O_4$ for $T > T_N$ is a pseudogapped one and is interpreted in the framework of 1D excitations before the onset of three-dimensional magnetic ordering [20]. As shown in Figs. 5 and 6, the inelastic neutron-scattering spectrum at 90 K of the $x = 0.3$ compound also exhibits a large pseudogapped feature at the same Q value as for $x = 0$, close to 1.25 Å^{-1}. In addition, as in the $x = 0$ case [20], this pseudogapped spectrum can be seen over a large temperature range, extending up to 150 K for $x = 0.3$. The Sc substitution affects several characteristics of the 1D excitation spectrum, however. The intensity of the excitation decreases with x, and the energy position of the intensity maximum E_0 increases: It is close to 11 meV at 90 K for $x = 0.3$, to be compared with the $E_0 \sim 8$ meV value observed in the $x = 0$ compound at the same temperature (Fig. 6). The temperature evolution of E_0, plotted for the $x = 0$, 0.2, and 0.3 compositions, is displayed in Fig. 7(a): It shows clearly that E_0 shifts towards higher energies as T increases (the so-called "blueshift" [29]) for the three compositions and that increasing x also increases E_0 for a given temperature. The Q width of this excitation is also clearly x dependent and becomes larger as x increases (Fig. 6, right panels).

It is in the LRO regime that the excitation spectra seem to be the most sensitive to dilution. The intensity of the magnetic scattering drops sharply, and in contrast with β-$CaCr_2O_4$, below 50 K, low-energy magnetic excitations can be seen in all substituted compounds from $x = 0.1$ to 0.3 (Fig. 5 and corresponding profiles in Fig. 6). As a result, the excitation spectra below the Néel ordering temperature of the substituted compounds ($x \leqslant 0.3$) remain dispersive but do not show the intensity maximum around 4 meV observed in the $x = 0$ case [20].

Increasing the substitution level to $x = 0.5$ and up to $x = 1$ (not shown), the excitation spectra become characteristic of disordered systems, with a broad quasielastic signal extending up to ~8 meV at 4 K (Fig. 5) and without any signature of propagating excitations (as illustrated in Figs. 5 and 6 for the $x = 0.5$ case). The $Q = 1.25$ Å^{-1} profile of this quasielastic scattering in Fig. 6 shows that the magnetic intensity below 8 meV increases slightly upon cooling, indicating a slowing down of the spin fluctuations. This profile is well described by a quasielastic Lorentzian $\omega\Gamma/(\omega^2 + \Gamma^2)$, which corresponds to the time-Fourier transform of an exponential relaxation process $\exp(-t/\tau)$ with $\tau \sim \Gamma^{-1}$. The resulting temperature evolution of the relaxation rate Γ is shown in Fig. 7(b) for $x = 0.5$: At $Q = 1.25$ Å^{-1}, Γ falls from ~9 meV at 90 K to ~3 meV below 18 K, remaining roughly constant upon further cooling. Although the magnetic response is fully dynamic above 30 K, the gradual increase in the magnetic elastic scattering as T decreases below 30 K [Fig. 7(b) and the inset of Fig. 4] signals the development of magnetic correlations on a time scale set by the energy resolution of the instrument ($\Delta E \sim 2$ meV, that is, $\tau > \hbar/\Delta E \sim 2.10^{-12}$ s). A similar behavior is observed for $x = 1$. The magnetic response of compounds $x = 0.5$ and up to $x = 1$ at 4 K can be therefore understood as the superposition of frozen (with respect to the neutron energy time scale) and still fluctuating disordered spins at this temperature.

Substitution in a zigzag chain has two effects: Because of dilution and cell volume increase, it weakens the average magnetic exchange in the system, an effect which is perceptible through the decrease in T_N, and it breaks the system into smaller units, provided that *two* defects are adjacent. The evolution of the average length of a zigzag chain versus x roughly follows a $l \sim 1/(x/2)^2$ law (see Fig. 1) as two contiguous defects are required to break the system connectivity, to be compared with $\sim 2/x$ for a single chain in which one defect is enough to break the connectivity (l is expressed as a number of contiguous Cr atoms, see Fig. 1). For $x = 0.3$, the correlation length determined from the width of the magnetic Bragg peak is on the order of 80 Å, which corresponds to ~55 Cr atoms, the expected calculated value being ~45 Cr atoms for a zigzag system [$l = 1/(0.3/2)^2$ according to the formula above] and only ~7 Cr atoms for a single chain ($l = 2/0.3$) for this level of substitution. This confirms the fact that the alternate magnetic pathways around the defects, provided by the zigzag ladder topology, are crucial at high substitution levels to maintain magnetic ordering below T_N and to allow the 1D magnetic excitation to propagate above. According to our results, the threshold size, below which characteristics of a SG system are experimentally observed, is therefore between 45 ($x = 0.3$) and 16 ($x = 0.5$) Cr atoms.

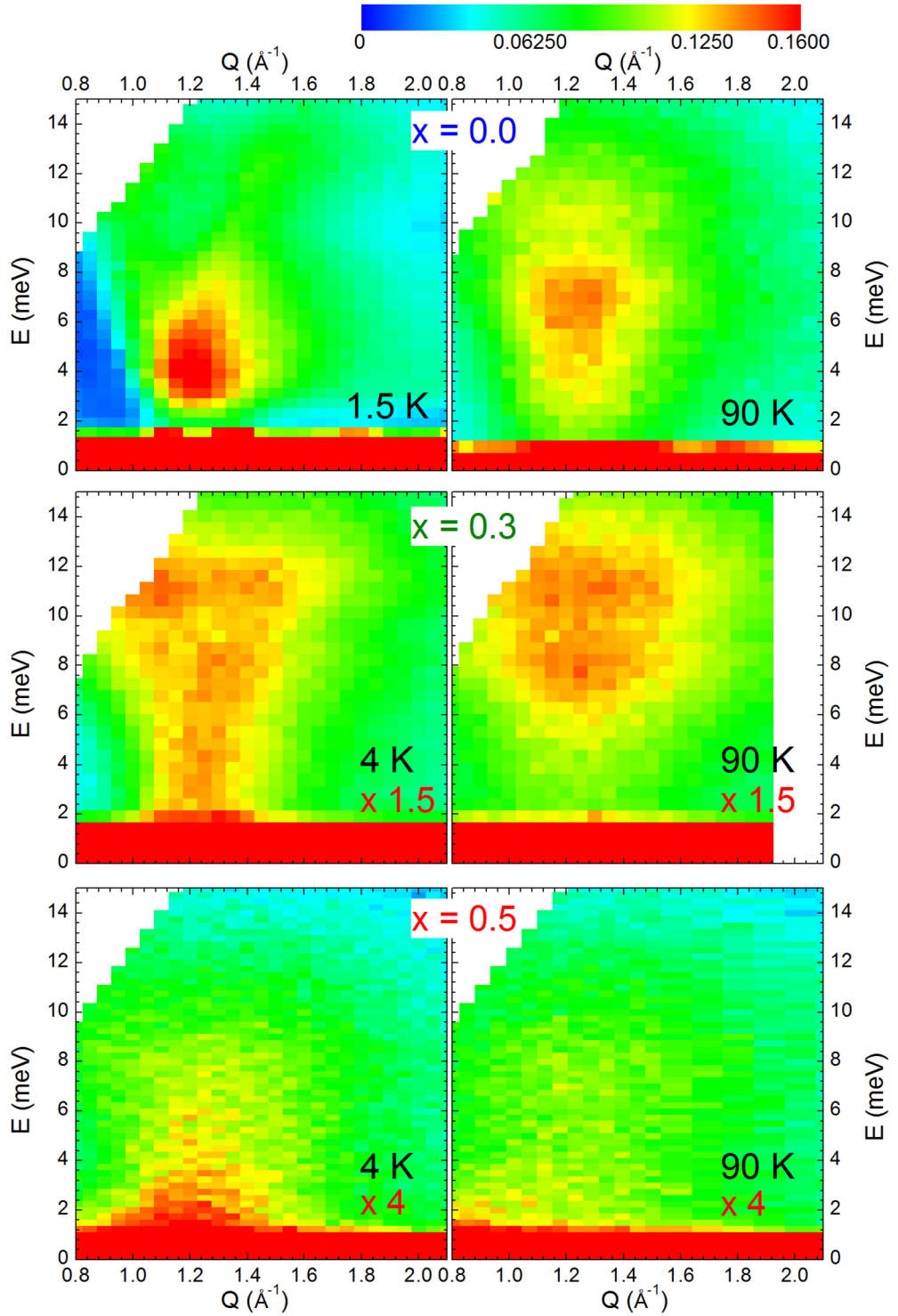

FIG. 5. (Color online) Inelastic neutron-scattering powder spectra of the $x = 0.0$, 0.3, and 0.5 compounds below 4 K and at 90 K. Data have been normalized with respect to the elastic incoherent scattering intensity. Intensity has been multiplied by 1.5 on the $x = 0.3$ maps and by 4 on the $x = 0.5$ maps to use the same color scale for all maps.

The increase in the pseudogap inferred from the increase in E_0 with increasing x in a $S = 3/2$ zigzag ladder is reported here. Mention of such a vacancy-induced blueshift can be found in the literature but always in the case of Haldane ($S = 1$) chains [29] for which numerical calculations have shown that the energy gap of a chain of length L actually increases with decreasing L [30]. Finite-size effects could also be invoked to explain the high-frequency shift of E_0 with x in the β-$CaCr_{2-x}Sc_xO_4$ system, but in the absence of a better understanding of the origin of the pseudogap in β-$CaCr_2O_4$, going further remains extremely speculative. Several hypotheses can be proposed to account for the

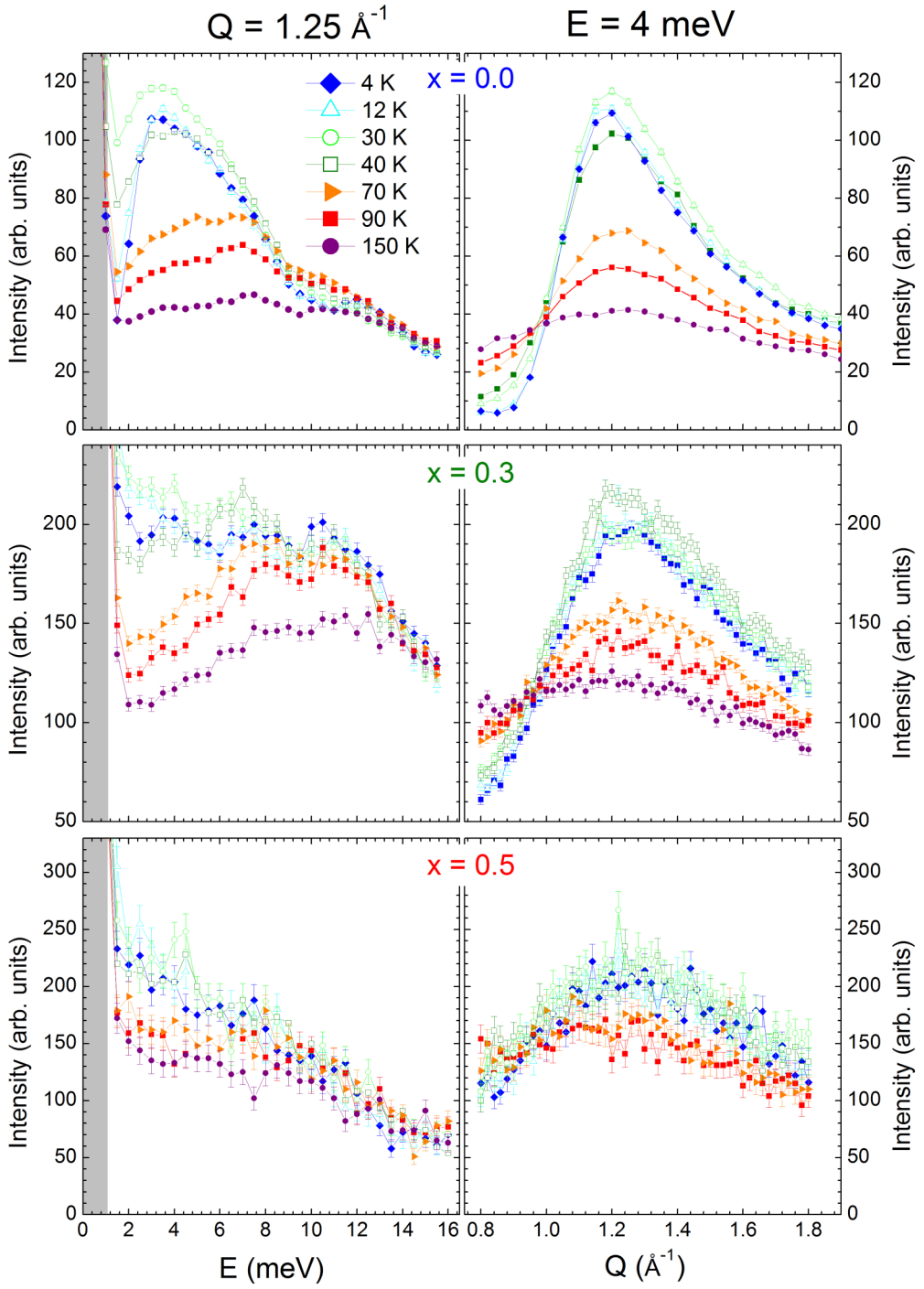

FIG. 6. (Color online) Constant $Q = 1.25$ Å^{-1} (left) and constant $E = 4$ meV (right) scans at several temperatures for $x = 0.0$, 0.3, and 0.5 in the β-$CaCr_{2-x}Sc_xO_4$ system (no Bose factor or background corrections have been applied).

pseudogap of the $x = 0$ phase: As discussed in Ref. [20], an additional interladder coupling J' cannot be ruled out. Because it is expected to decrease magnetic couplings, it is not clear in this case how dilution would lead to an increase in the gap, unless only finite-size effects are considered. Regardless of the strength and the sign of J_1, an extremely small alternation of the J_2 value induced by Ca substitution on the Sr site has been seen experimentally to induce a spin gap of about ∼4 meV in the excitation spectrum of the customary gapless $S = \frac{1}{2}$ chain system $SrCuO_2$ [31]. Similarly, alternation of J_1 also leads to a gapped ground state [6]: Bearing in mind the magnetoelastic effect observed below 150 K in β-$CaCr_{2-x}Sc_xO_4$ compounds up to $x = 0.3$, a distribution of the Cr-Cr distances in the ladder could also lead to a gapped ground state. Furthermore, according to recent results on the Ni substitution on the magnetic Cu site in $SrCuO_2$ [9], a pseudogap could even be a generic feature of quantum spin chains with dilute defects. Accordingly, 1% chemical defects in the Cr site could lead to

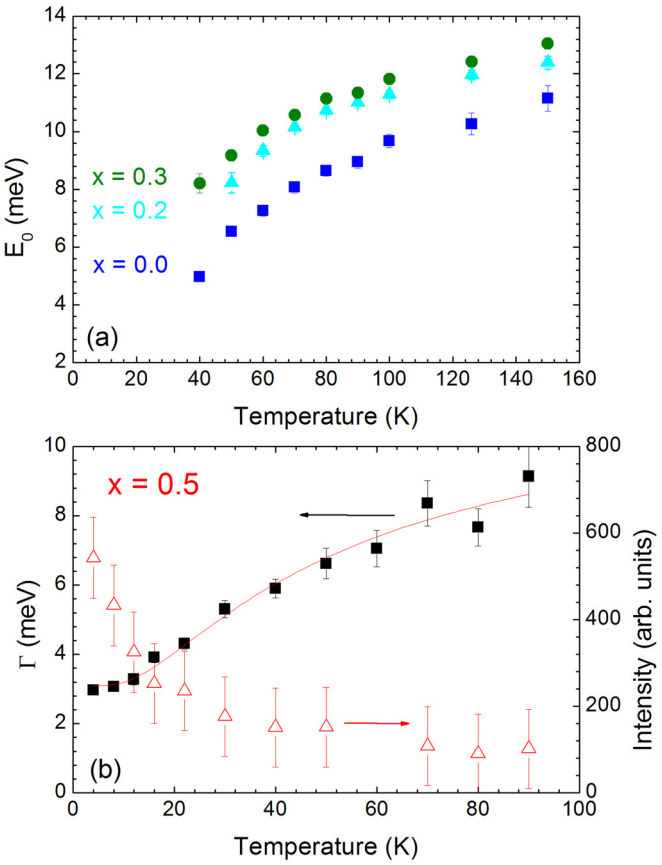

FIG. 7. (Color online) (a) Temperature dependence of the characteristic energy E_0 of the pseudogapped magnetic excitation for $x = 0, 0.2$, and 0.3. (b) Evolution with temperature of the relaxation time Γ (left scale) and of the integrated elastic magnetic intensity (right scale) for $x = 0.5$. The red line is a guide to the eye.

a pseudogapped excitation in β-$CaCr_2O_4$ without it being intrinsic to the magnetic topology. In this respect, studying the β-$(Ca,Sr)Cr_2O_4$ system would provide key information on the impact of the alternation of the exchange couplings on a zigzag ladder and might lead to a better understanding of the origin of the pseudogap.

IV. CONCLUSION

To summarize, the magnetic phase diagram of the $S = 3/2$ zigzag ladder system β-$CaCr_{2-x}Sc_xO_4$ system has been established through the combined use of elastic, inelastic neutron-scattering experiments, magnetic susceptibility, and specific heat measurements. It shows that the pseudogapped excitation seen in $x = 0$ still persists up to high dilution levels ($x \leqslant 0.3$), despite the weakened magnetic interactions and the reduced magnetic order correlation length. As x increases, both an increase in the energy E_0 of the excitation, and a broadening in its Q profile are observed. For $x \geqslant 0.5$, which corresponds to an average chain length of $\leq$16 Cr atoms, the system enters a disordered state with glasslike dynamics at low temperatures. The high threshold substitution level, below which 1D characteristics are still observed, is a result of the zigzag ladder topology, which allows alternate exchange paths around defects, in contrast with simple magnetic chains.

ACKNOWLEDGMENTS

The authors are grateful to Dr. G. Roux for fruitful discussions. Special acknowledgment is due Dr. E. Elkaïm at the Soleil Synchrotron (Saint-Aubin, France) for the synchrotron x-ray powder diffraction experiments versus temperature and to Dr. E. Suard at ILL (Grenoble, France) for room-temperature high-resolution neutron-diffraction data.

[1] J. Cloizeaux and J. Pearson, Phys. Rev. **128**, 2131 (1962).
[2] J. W. Bray, H. R. Hart, L. V. Interrante, I. S. Jacobs, J. S. Kasper, G. D. Watkins, S. H. Wee, and J. C. Bonner, Phys. Rev. Lett. **35**, 744 (1975).
[3] M. Hase, I. Terasaki, and K. Uchinokura, Phys. Rev. Lett. **70**, 3651 (1993).
[4] T. Hikihara, M. Kaburagi, and H. Kawamura, Phys. Rev. B **63**, 174430 (2001).
[5] R. Roth and U. Schollwöck, Phys. Rev. B **58**, 9264 (1998).
[6] H.-J. Mikeska and A. Kolezhuk, *Quantum Magnetism*, Lecture Notes in Physics Vol. 645 (Springer-Verlag, Berlin/Heidelberg, 2004), pp. 1–83.
[7] M. Azuma, Z. Hiroi, M. Takano, K. Ishida, and Y. Kitaoka, Phys. Rev. Lett. **73**, 3463 (1994).
[8] R. S. Eccleston, T. Barnes, J. Brody, and J. W. Johnson, Phys. Rev. Lett. **73**, 2626 (1994).
[9] G. Simutis, S. Gvasaliya, M. Månsson, A. L. Chernyshev, A. Mohan, S. Singh, C. Hess, A. T. Savici, A. I. Kolesnikov, A. Piovano, T. Perring, I. Zaliznyak, B. Büchner, and A. Zheludev, Phys. Rev. Lett. **111**, 067204 (2013).
[10] Y. Endoh, I. U. Heilmann, R. J. Birgeneau, G. Shirane, A. R. McGurn, and M. F. Thorpe, Phys. Rev. B **23**, 4582 (1981).
[11] S. E. Nagler, W. J. L. Buyers, R. L. Armstrong, and R. A. Ritchie, J. Phys. C: Solid State Phys. **17**, 4819 (1984).
[12] I. Y. Korenblit and E. F. Shender, Phys. Rev. B **48**, 9478 (1993).
[13] M. Thede, F. Xiao, C. Baines, C. Landee, E. Morenzoni, and A. Zheludev, Phys. Rev. B **86**, 180407 (2012).
[14] C. L. Kane and M. P. A. Fisher, Phys. Rev. Lett. **68**, 1220 (1992).
[15] Y. Imry, P. A. Montano, and D. Hone, Phys. Rev. B **12**, 253 (1975).
[16] A. Lavarélo and G. Roux, Phys. Rev. Lett. **110**, 087204 (2013).
[17] D. S. Fisher, Phys. Rev. B **50**, 3799 (1994).
[18] M. Azuma, Y. Fujishiro, M. Takano, M. Nohara, and H. Takagi, Phys. Rev. B **55**, R8658 (1997).
[19] F. Damay, C. Martin, V. Hardy, A. Maignan, G. Andre, K. Knight, S. R. Giblin, and L. C. Chapon, Phys. Rev. B **81**, 214405 (2010).
[20] F. Damay, C. Martin, V. Hardy, A. Maignan, C. Stock, and S. Petit, Phys. Rev. B **84**, 020402(R) (2011).
[21] F. D. M. Haldane, Phys. Rev. B **25**, 4925 (1982).
[22] S. R. White and I. Affleck, Phys. Rev. B **54**, 9862 (1996).
[23] S. E. Dutton, C. L. Broholm, and R. J. Cava, J. Solid State Chem. **183**, 1798 (2010).
[24] W. Horkner and H. Mullerbuschbaum, Z. Naturforsch. B **31**, 1710 (1976).

[25] H. Mullerbuschbaum and H. Schnering, Z. Anorg. Allg. Chem. **336**, 295 (1965).
[26] R. Shannon and C. Prewitt, Acta Crystallogr., Sect. B: Struct. Crystallogr. Cryst. Chem. B **25**, 925 (1969).
[27] J. Rodriguez-Carvajal, Physica B **192**, 55 (1993).
[28] J. A. Mydosh, *Spin Glasses* (Taylor & Francis, London, 1993).
[29] M. Kenzelmann, G. Xu, I. A. Zaliznyak, C. Broholm, J. F. DiTusa, G. Aeppli, T. Ito, K. Oka, and H. Takagi, Phys. Rev. Lett. **90**, 087202 (2003).
[30] S. R. White, Phys. Rev. Lett. **69**, 2863 (1992).
[31] F. Hammerath, S. Nishimoto, H.-J. Grafe, A. U. B. Wolter, V. Kataev, P. Ribeiro, C. Hess, S.-L. Drechsler, and B. Büchner, Phys. Rev. Lett. **107**, 017203 (2011).